

OPEN ACCESS

EDITED BY

Peng Lv,

Hebei Academy of Agricultural and Forestry Sciences. China

REVIEWED BY

Chokri Hafsi

Biotechnology Center of Borj Cedria (CBBC); Higher Institute of Biotechnology of Beja (ISBB), Tunisia

Yongfu Tao,

Chinese Academy of Agricultural Sciences, China

*CORRESPONDENCE

Yufei Zhou

xhouyf19@126.com

RECEIVED 11 July 2025 ACCEPTED 30 September 2025 PUBLISHED 21 October 2025

CITATION

Liu C, Liu S, Hu X, Shi X, Liu C, Sun L and Zhou Y (2025) Hydrogen sulfide enhances salt tolerance in sorghum by activating the chloroplastic AsA–GSH cycle to sustain photosynthesis.

Front. Plant Sci. 16:1664076. doi: 10.3389/fpls.2025.1664076

COPYRIGHT

© 2025 Liu, Liu, Hu, Shi, Liu, Sun and Zhou. This is an open-access article distributed under the terms of the Creative Commons Attribution License (CC BY). The use, distribution or reproduction in other forums is permitted, provided the original author(s) and the copyright owner(s) are credited and that the original publication in this journal is cited, in accordance with accepted academic practice. No use, distribution or reproduction is permitted which does not comply with these terms.

Hydrogen sulfide enhances salt tolerance in sorghum by activating the chloroplastic AsA—GSH cycle to sustain photosynthesis

Chang Liu¹, Sitong Liu¹, Xin Hu¹, Xiaolong Shi¹, Chunjuan Liu¹, Lu Sun² and Yufei Zhou^{1*}

¹College of Agronomy, Shenyang Agricultural University, Shenyang, China, ²College of Life Engineering, Shenyang Institute of Technology, Shenyang, China

Soil salinization poses a severe threat to global food security by reducing crop productivity, particularly in semi-arid regions where sorghum (Sorghum bicolor L.) is a major cereal crop. Hydrogen sulfide (H₂S) has recently been recognized as a signaling molecule involved in plant stress tolerance. However, its role in regulating the chloroplastic ascorbate-glutathione (AsA-GSH) cycle and photosynthetic performance in sorghum under salt stress remains unclear. To investigate the potential regulatory role of exogenous H₂S, sorghum seedlings were subjected to salt stress with or without sodium hydrosulfide (NaHS, an H₂S donor). Physiological, biochemical, and chlorophyll fluorescence parameters were assessed to evaluate growth performance, antioxidant capacity, and photosynthetic responses. The concentrations of reduced and oxidized forms of ascorbate (AsA/DHA) and alutathione (GSH/GSSG), together with the activities of key enzymes in the AsA-GSH cycle, were determined. Salt stress significantly inhibited sorghum seedling growth, enhanced reactive oxygen species (ROS) accumulation, and disrupted redox homeostasis. Exogenous H₂S alleviated these effects by stimulating the AsA-GSH cycle in chloroplasts. H₂S treatment maintained higher levels of reduced AsA and GSH while promoting moderate accumulation of DHA and GSSG, accompanied by elevated activities of ascorbate peroxidase (APX), glutathione reductase (GR), dehydroascorbate reductase (DHAR), and monodehydroascorbate reductase (MDHAR). Moreover, H₂S improved photosynthetic performance by maintaining chlorophyll content and chloroplast ultrastructure, optimizing chlorophyll fluorescence parameters, and protecting photosystem II (PSII) from photoinhibition. Enhanced electron transfer from the PSII reaction center to plastoquinone further indicated an improved capacity for energy dissipation under salt stress. These findings demonstrate that exogenous H₂S confers salt tolerance in sorghum by activating the chloroplastic AsA-GSH redox cycle and preserving photosynthetic efficiency. The study highlights H_2S as a critical mediator of chloroplast redox regulation, providing an effective strategy for enhancing sorghum resilience to soil salinization and promoting sustainable agricultural production.

KEYWORDS

sorghum, salt stress, hydrogen sulfide, AsA-GSH cycle, photosynthesis

1 Introduction

Soil salinization, a consequence of irrigation practices, climate change, and natural soil processes, has become a major threat to global food security by severely impacting crop productivity (Mishra et al., 2023). Salinity stress restricts crop productivity by inducing osmotic stress and ion toxicity, which disrupt water uptake, ion homeostasis, photosynthesis, and ultimately reduce growth and yield (Parihar et al., 2015). Sorghum (Sorghum bicolor L.), an important cereal crop known for its tolerance to various environmental stresses, is predominantly cultivated in regions prone to salt-affected soils (Liu et al., 2023; Wei et al., 2024). Salinity hampers sorghum growth by disrupting essential physiological processes, including photosynthesis (Rajabi Dehnavi et al., 2022; Yang et al., 2020) and antioxidant metabolism (Chen et al., 2022; Guo et al., 2022), leading to reduced yields and potential crop failures. During crop adaptation to salinity stress, the identification and exploitation of salt-tolerance genes-such as the TALE (Liang et al., 2025), the CASPL (Xue et al., 2024a, 2024b), and the RALF (Xue et al., 2024c) and TEF (Liu et al., 2024)—constitute a pivotal strategy for breeding salt-tolerant cultivars. At same time, the exogenous application of plant growth regulators represents another critical approach for modulating sorghum salt tolerance.

The photosynthetic apparatus is a primary target in plants under salt stress, with the thylakoid membrane and associated electron transport components being particularly sensitive (Zhang et al., 2010). Within the chloroplast, the AsA-GSH cycle acts as a shield for photosynthesis against the oxidative harm triggered by salt stress (Tan et al., 2022). Beyond enhancing plant resilience across various stress scenarios (Zhu et al., 2022), this cycle also plays a key role in scavenging reactive oxygen species (ROS) within plant cells (Wu et al., 2019). However, under salt stress, the AsA-GSH cycle in plants is significantly impaired (Prajapati et al., 2023), adversely affecting crucial cellular activities such as stomatal movement (Khan et al., 2021). Notably, Hydrogen sulfide (H₂S) can counteract salt stress by activating antioxidants within the AsA-GSH cycle and boosting the ROS scavenging ability within wheat plant cells (Kaya et al., 2023). However, the precise regulatory mechanisms by which H₂S influences the photosynthetic process and the antioxidant metabolic pathways in sorghum seedlings remain to be elucidated.

Hydrogen sulfide (H₂S), an emerging gasotransmitter with significant physiological functions in plants, has demonstrated potential in modulating plant responses to abiotic stresses (Xuan et al., 2020). Functioning as a signaling molecule, H₂S participates in a variety of plant processes, including regulating gene expression, modifying proteins post-translationally, and preserving cellular redox balance (Alvi et al., 2023). Recent studies have highlighted that H₂S could be crucial in enhancing plant resilience to adverse stress by regulating antioxidant defense mechanisms and safeguarding photosynthetic machinery. For instance, exogenous H₂S application can improve cabbage photosynthesis under black rot stress by reducing chlorophyll degradation, enhancing gas exchange, and upregulating Calvin cycle enzyme activities and gene expressions related to photosynthesis (Wang et al., 2024). In

addition, exogenous application of H2S, has been widely employed to enhance drought tolerance in plants. Such treatments promote the accumulation of polyamines, soluble sugars, and glycine betaine, while simultaneously stimulating antioxidant enzyme activities. These changes collectively mitigate drought-induced osmotic and oxidative stress, thereby improving the adaptive capacity of plants under adverse conditions (Thakur et al., 2021). Cui et al. (2025) indicated that H₂S enhances plant cold tolerance by activating antioxidant defense mechanisms and facilitating the accumulation. In addition, exogenous iron and H2S collectively enhance seedling growth, maintain pigment composition, and bolster the antioxidative defense system in tomato seedlings under NaCl stress by increasing endogenous H2S content and Lcysteine desulfhydrase activity (Subba et al., 2023). Also, exogenous H₂S has been demonstrated to mitigate salt stress in cucumber seedlings through multiple mechanisms, including boosting photosynthesis, maintaining the AsA-GSH cycle, protecting mineral ion intake, reducing the Na⁺/K⁺, and activating the SOS and MAPK signaling pathways ((Luo et al., 2023). Thus, there is a significant interest in elucidating the role of H2S in regulating the physiological functions in sorghum under salt stress conditions.

The primary objectives of this experiment were to: (1) investigate how H_2S influences the growth of sorghum seedlings under salt stress conditions; (2) determine the impact of H_2S on the photosynthetic machinery; (3) examine the influence of H_2S on the AsA-GSH cycle in chloroplasts, which serves as a vital antioxidant defense system. By elucidating these mechanisms, our research seeks to provide essential insights for developing strategies to improve crop resilience against soil salinization, ultimately contributing to crop production and sustainable agriculture.

2 Materials and methods

2.1 Experimental location

The experiment was carried out within an artificial climate chamber (model AR-41L3 Flex, Percival, HK) situated in the Sorghum Physiology Laboratory at the Agronomy College, Shenyang Agricultural University. Specifically, the experimental chamber was set to maintain a consistent temperature of 28°C throughout both day and night, with a photoperiod set at 12 hours, an illumination intensity of 280 $\mu mol\ m^{-2}s^{-1}$, and a relative humidity at 84%.

2.2 Experimental materials and design

Sorghum inbred line, SX44B, was utilized as the experimental material in this study. Homogeneous sorghum seeds were meticulously chosen and sanitized using a 5% sodium hypochlorite solution for a duration of 10 minutes, after which they were placed in Petri dishes. Subsequently, the seeds were germinated in an incubator with a constant temperature value maintained at 25°C for a period of 3 days. After germination,

seedlings that exhibited robust growth were transferred into hydroponic boxes, with 16 seedlings per box. The seedlings were initially cultured in distilled water for 3 days, before being transferred to a 1/2 Hoagland nutrient solution for an additional 3 days. Upon reaching the stage where second sorghum seedling leaf fully expanded, they were exposed to stress treatment with a 200 mmol/L NaCl salt solution (Yu et al., 2025). Sodium hydrosulfide (NaHS) at a concentration of 50 µmol/L was used as a hydrogen sulfide (H₂S) donor, and hypotaurine at 0.1 mmol/L served as an H₂S scavenger (based on previous results). Following salt stress, H₂S or the H₂S scavenger was sprayed once daily for the three consecutive days, with each application consisting of 8 mL. The experiment consisted of five treatments: (1) plants not exposed to salt stress received an equivalent volume of distilled water (CK), (2) plants not exposed to salt stress and treated with H_2S (CK+ H_2S), (3) salt-stressed plants that were sprayed with distilled water (S), (4) salt-stressed plants that were sprayed with H₂S (S+H₂S), and (5) salt-stressed plants that were sprayed with both H2S and the H2S scavenger (S+H₂S+HT). Throughout the experiment, the nutrient solution was refreshed every three days, and after a 7-day period of salt stress, uniform sorghum seedlings were selected for the measurement of various parameters (Tao et al., 2021).

2.3 Morphological measurements

Uniformly developed plant seedlings were selected from each treatment and cleaned with distilled water. The moisture on the surface of seedlings was carefully removed using filter paper. Subsequently, the shoot and root parts were dissected using scissors. The lengths of both the shoot and root sections were then precisely measured with a calibrated ruler. The fresh weights of these parts were accurately determined using an electronic balance accurate to 0.001 grams. Following this, each part was individually placed into a brown paper envelope and subjected to drying in an oven at 80°C until reaching a constant weight. Ultimately, the dry weights of the shoots and roots were then measured, with three replicates for each treatment (Yu et al., 2024).

2.4 Determination of MDA and reactive oxygen species content

The determination of O₂ content followed the method described by (Luo et al., 2023). Specifically, 0.5 g of the first fully expanded leaves from sorghum seedlings were collected in an ice bath and homogenized in 2 mL of extraction buffer. The mixture was then centrifuged at 8000×g for a duration of 10 minutes at 4°C, and the resulting supernatant was carefully retrieved. Next, Subsequently, 1 mL of the supernatant was combined with 0.5 mL of phosphate buffer (50 mmol/L, pH 7.8) and 0.1 mL of hydroxylamine hydrochloride chemical solution (10 mmol/L), and the reaction mixture was shaken and incubated at 25°C for 20 minutes. Subsequently, the mixture was treated with 1 mL of para-aminobenzenesulfonic acid solution (58 mmol·L⁻¹) and 1 mL

of α -naphthylamine solution (7 mmol·L⁻¹). After adding these reagents, the mixture was thoroughly combined and subjected to oscillation at 30 °C for a period of 30 minutes. Ultimately, an equal volume of chloroform was introduced into the mixture, which was then subjected to centrifugation at 10,000×g for 3 minutes. The supernatant was carefully extracted, and its absorbance was assessed at a wavelength of 530 nm. The concentration of O_2 was subsequently quantified by referring to a pre-established standard calibration curve.

The $\rm H_2O_2$ content was determined according to the procedure reported by Moloi and van der Westhuizen (2006). Specifically, 0.1 g of the first fully expanded leaves from sorghum seedlings were ground in 5 mL of cold acetone. The resulting homogenate was centrifuged at 4°C for 15 minutes, and the supernatant was carefully decanted. To this supernatant, 0.5 mL of titanium tetrachloride (TiCl₄) reagent was added. During the mixing process, 3.5 mL of 25% ammonium hydroxide (NH₄OH) was added dropwise. The mixture was then centrifuged again at 4°C for 5 minutes. The supernatant was discarded, and the precipitate was washed thoroughly with 5 mL of acetone until it turned colorless. Finally, the precipitate was melted in NH₂SO₄ solution (20 mL), and the absorbance was determined at 415 nm.

Nitroblue Tetrazolium (NBT) and Diaminobenzidine (DAB) Staining: Leaf segments (6–8 cm) from the first fully expanded leaves of sorghum seedlings were collected, with four replicates per treatment. Samples were incubated in NBT or DAB solution in the dark at room temperature for 6 h, followed by decolorization in 95% ethanol at 40 °C for 16 h. The decolorized leaves were rinsed, blotted dry, and photographed.

The malondialdehyde (MDA) content was assessed using the thiobarbituric acid (TBA) method, as described by Jin et al. (2020). Specifically, a 0.5 g sample of the first fully expanded leaves from sorghum seedlings was homogenized in trichloroacetic acid (5 mL) while being kept in an ice bath to ensure low-temperature conditions. After homogenization, the mixture was centrifuged at 8000×g for 15 minutes at 4°C to separate the components. Next, the resulting supernatant (2 mL) was combined with 5 mL TBA solution (0.67%) and incubated in boiling water for 30 minutes, after which it was cooled in an ice bath. The mixture was then subjected to centrifugation at 10000×g at 4°C for 15 minutes. Finally, the absorbance was determined at wavelengths of 532 nm, 600 nm, and 450 nm, respectively, using a 0.67% TBA solution as the reference.

The determination of MDA content is expressed through the following formula:

MDA (μ mol/g FW) = 6.45 × (A532 – A600) – 0.56 × A450

where A450, A532, and A600 denote the optical density readings at 450 nm, 532 nm, and 600 nm, respectively.

2.5 Chloroplast extraction and preparation

The extraction and preparation of chloroplasts from leaf tissues were conducted in accordance with the protocol detailed by

Bhattacharya et al. (2020). The first fully expanded leaves were selected (1 g), washed, and dried to remove petioles and major veins. The leaves were then homogenized in phosphate buffer (2 mL) and passed through a 100 μ m mesh filter. The filtrate underwent centrifugation at 3000×g for 10 minutes on two separate occasions. Following each centrifugation, the supernatant was removed, and the resulting pellet was retained. Further centrifugation was conducted at 200×g and 1000×g for 2 minutes respectively, and the pellets were discarded while the supernatant was taken. Finally, the supernatant was subjected to centrifugation at 3000×g for 10 minutes, and the resulting pellet was collected as the chloroplast fraction. The chloroplasts were resuspended in 400 μ L of chloroplast suspension solution for use in subsequent experiments.

2.6 Determination of antioxidant substances in the AsA-GSH cycle

A 300 μ L aliquot of chloroplast suspension was mixed with 1.2 mL of 6% perchloric acid that had been pre-cooled. This mixture was then processed via centrifugation at 14000×g for 10 minutes at a temperature of 4°C. The concentrations of Ascorbic acid (AsA) and Dehydroascorbic acid (DHA) were assessed using the technique detailed by Wang et al. (2012). In parallel, to measure the levels of Glutathione (GSH) and Oxidized glutathione (GSSG), another 300 μ L of chloroplast suspension was combined with 1.2 mL of 5% sulfosalicylic acid and subjected to centrifugation under identical conditions.

2.7 Determination of antioxidant substances enzyme activities in the AsA-GSH cycle

The assays for antioxidant enzyme activities within the AsA-GSH cycle were conducted following the protocols provided by the respective commercial kits. Specifically, the chloroplast suspension was carefully decanted into a fresh centrifuge tube. The kits utilized for measuring Ascorbate peroxidase (APX), Glutathione reductase (GR), Dehydroascorbate reductase (DHAR), and Monodehydroascorbate reductase (MDHAR) were procured from Suzhou Greats Biotech Co., Ltd., located in Suzhou, China.

2.8 Observation of chloroplast ultrastructure

Before collecting the samples, the leaves were thoroughly rinsed with distilled water, and any residual surface moisture was gently absorbed using filter paper. Next, the leaves were carefully excised into slender strips, approximately $1~\mathrm{mm} \times 3~\mathrm{mm}$ in dimension, using a sharp blade (while avoiding the veins), and stored in glass vials filled with 2.5% pentanediol. To ensure complete submersion

of the leaves in the glutaraldehyde solution, the vials were carefully depressurized using a syringe. Subsequently, they were kept at a refrigerated temperature of 4°C for the fixation process. After 2 days, the samples underwent three successive rinses with phosphate buffer (pH 7.8), fixed in osmium tetroxide (1%) for 2 hours, rinsed again three times with phosphate buffer, and then subjected to a dehydration process (50% and 70% ethanol, 80% and 90% acetone, each concentration for 15 minutes, and finally treated three times with 100% acetone, each time for 30 minutes). Subsequently, the samples were embedded in a blend composed of epoxy propane and SPON-812, followed by polymerization in a controlled environment chamber for a duration of 12 hours. The samples were meticulously sliced into 50 nm ultra-thin sections utilizing a Leica EM UC7 ultramicrotome (Wetzlar, Germany). These sections were subsequently mounted onto copper grids and subjected to staining with uranyl acetate and lead citrate solutions. Finally, the detailed structural analysis was conducted using a Zeiss LSM 500 transmission electron microscope (Zeiss, Germany).

2.9 Determination of chlorophyll synthesis precursors

The quantification of 5-Aminolevulinic acid (ALA) was conducted according to the method outlined by Wang et al. (2021). Specifically, 2 g of the first fully expanded leaves from sorghum seedlings were ground in 6 mL of ice-cold acetic acid buffer (pH 4.6) and then centrifuged at 5000×g for 15 minutes at 4°C. 4 mL of the resulting supernatant were combined with 100 μL of ethyl acetate and incubated at 100°C for 10 minutes. An equal volume of Ehrlich's reagent, which consists of 2% p-dimethylaminobenzaldehyde, 6% perchloric acid, and 88% acetic acid, was added. After a 10-minute incubation, the absorbance was measured at 554 nm.

The measurement of porphobilinogen (PBG) content was adapted from the protocol described by Bogorad (1962) with slight adjustments. In detail, 0.3 g of the first fully expanded leaves from sorghum seedlings were carefully removed, finely minced, and transferred to a mortar. The leaf tissue was then homogenized with 2 mL of extraction buffer (0.6 mol/L Tris-HCl, 0.1 mol/L EDTA, pH 8.2) while kept in an ice bath until a homogeneous mixture was achieved. This homogenate was subsequently transferred to a centrifuge tube and centrifuged at 12000×g for 15 minutes. The supernatant was carefully collected, and an equal volume of Ehrlich's reagent was added. After incubating in the dark for 15 minutes, the absorbance was recorded at 553 nm.

To determine the levels of protoporphyrin IX (Proto IX), Mg-protoporphyrin (Mg-Proto IX), and protochlorophyllide (Pchl), 0.3 g of the first fully expanded leaves from sorghum seedlings were chosen and homogenized in a mortar with 25 mL basic acetone (80%). Following the removal of impurities through filtration, the absorbance was determined at 575 nm, 590 nm, and 628 nm, respectively. The concentrations were then calculated using the equations provided by Wu et al. (2018).

2.10 Determination of photosynthetic pigments

Uniform plants from each treatment were selected, and the first fully expanded leaves were selected. The leaf surface was cleaned thoroughly, after which the leaves were cut into smaller sections. Subsequently, 0.1 g of fresh leaves were weighed for each replicate, with a total of three replicates for each treatment. Samples were positioned in glass containers and fully immersed in 10 mL ethanol (95%). The containers were stored in complete darkness for 48 hours to facilitate the complete extraction of chlorophyll. Subsequently, the analysis was performed using a UV-VIS spectrophotometer (Tokyo, Japan). The specific wavelengths corresponding to the maximum absorption peaks for chlorophyll a, chlorophyll b, and carotenoids in 95% ethanol were identified as 665 nm, 649 nm, and 470 nm, respectively.

The formulas used for calculations are as follows:

Concentration of chlorophyll a(mg · g⁻¹FW): Ca = 13.95A665 - 6.8A649

Concentration of chlorophyll b(mg \cdot g⁻¹FW): Cb = 24.96A649 - 7.32A665

Concentration of carotenoids(mg \cdot g⁻¹FW): Cc = (1000A470 - 2.05Ca - 114.8Cb)/248

Where A665 and others indicate the optical density of chlorophyll solutions at 665 nm, 649 nm, and 470 nm, respectively.

2.11 Determination of photosynthetic parameters

The core photosynthetic metrics assessed included the net photosynthetic rate (Pn), stomatal conductance (Gs), transpiration rate (Tr), and intercellular CO₂ concentration (Ci). These measurements were obtained from the first fully expanded leaf of sorghum seedlings, utilizing a Li-6400 photosynthesis system (LI-COR, USA). Each treatment was assessed with four replicates. The measurement conditions were standardized to a light intensity of 1000 μ mol·m $^{-2}$ ·s $^{-1}$, a CO₂ concentration of 385 \pm 5 μ mol·mol $^{-1}$, and a temperature of 28°C.

2.12 Assessment of chlorophyll fluorescence characteristics

For the assessment, the topmost fully expanded leaf was chosen, with four replicates for per treatment. Following a thorough rinse with distilled water and gentle drying of surface moisture using blotting paper, the leaves were acclimated in the dark at ambient temperature for 30 minutes. Leaf images were captured by a FlourCam FC800-O/2020 chlorophyll fluorometer (Brno, Czech Republic). The experimental setup for fluorescence measurements was configured in this manner: the initial fluorescence (F0) was captured under low

actinic light intensity of 0.1 μ mol·m-²·s-¹. This was succeeded by a saturation pulse light (10000 μ mol·m-²·s-¹ for 0.7 seconds) to measure the maximum fluorescence (Fm). Following a 15-minute acclimation period under a light intensity of 800 μ mol·m-²·s-¹, the value of Fm' was determined. From these readings, several essential parameters were extracted, including F0, Fm, the quantum efficiency of PSII (Fv/Fm), and non-photochemical quenching (NPQ).

2.13 OJIP curve and PQ pool measurement

The topmost fully expanded leaf was employed to assess chlorophyll fluorescence parameters, including OJIP curve and PQ pool, utilizing a DUAL-PAM-100 dual-channel fluorometer (WALZ, Germany). The measurements were conducted after the leaves had been dark-adapted for 30 minutes.

2.14 Statistical analysis

Data were organized using Excel 2021, and graphs were created with Graph Pad Prism 8. The data obtained from a minimum of three replicates are presented as mean \pm SD. Variance analysis was conducted using SPSS 26.0, and differences between treatments were tested for significance using Duncan's method. Differences among treatments that are statistically significant at the p< 0.05 level are denoted by distinct lowercase letters.

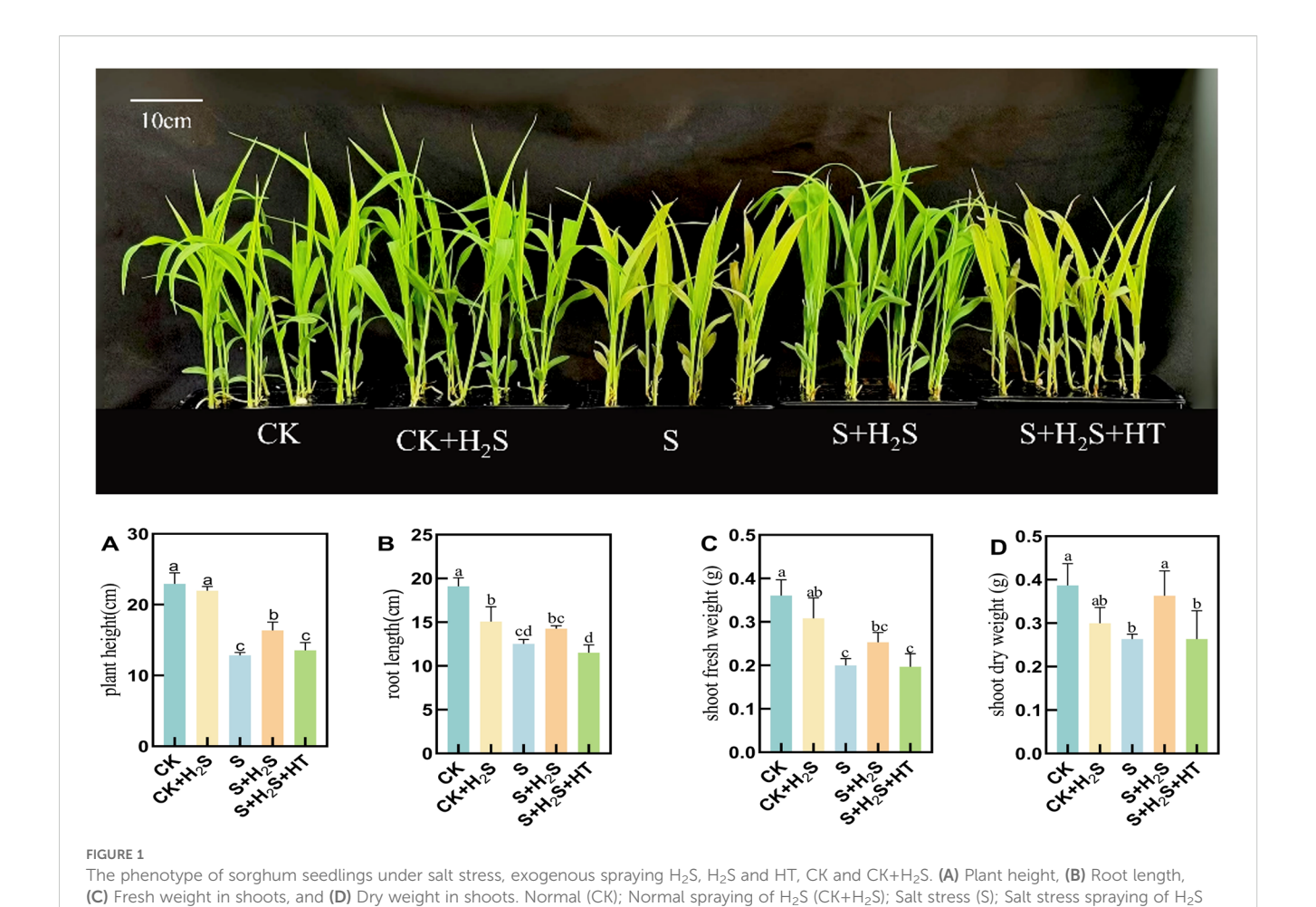
3 Results

3.1 Effect of exogenous H₂S on the morphology of sorghum seedlings

Sorghum seedlings under salt stress exhibited a marked decline in growth (Figure 1). Specifically, compared to CK, salt-treated seedlings experienced substantial reductions in plant height (44.04%), root length (34.38%), shoot fresh weight (44.54%), and shoot dry weight (31.9%). In comparison with the S treatment, the S+H₂S treatment increased the plant height, root length, shoot fresh weight, and shoot dry weight of the sorghum seedlings by 27.53%, 13.83%, 26.5%, and 37.97%, respectively. The S+H₂S+HT treatment resulted in a decrease in plant height, root length, shoot fresh weigh, and shoot dry weight by 17.31%, 19.93%, 22.13%, and 27.52% compared to the S+H₂S treatment. The aforementioned results indicated that foliar application of H₂S significantly mitigated the adverse effects of salt stress on the growth of sorghum seedlings, thereby enhancing their overall development.

3.2 Effect of exogenous H₂S on active oxygen species and MDA content of sorghum seedlings

To directly visualize the production of ROS in sorghum seedling leaves caused by salt stress, this study employed DAB and NBT staining



(S+H₂S); Salt stress spraying of H₂S and H₂S scavengers (S+H₂S+HT). The data represented the mean of the three replicates, and the different lower-

solutions to specifically stain tissues containing H_2O_2 and O_2^- in the sorghum seedling leaves. The intensity of leaf color correlates with the concentration of H_2O_2 and O_2^- , where a deeper color indicates higher levels of these reactive oxygen species. Compared to the CK, the S treatment significantly increased the content of O_2^- , H_2O_2 , and MDA in the sorghum seedling leaves by 129%, 56.56%, and 132.61%, respectively (Figure 2). In contrast, the S+H₂S treatment significantly reduced the content of O_2^- , H_2O_2 , and MDA by 47.47%, 19.47%, and 28.88%, respectively, compared to the S treatment. Furthermore, the S+H₂S+HT treatment resulted in notable increases in the content of O_2^- , H_2O_2 , and MDA by 20.54%, 22.54%, and 40.29%, respectively, compared to the S+H₂S treatment.

case letters represented a significant difference at the 5% level (P<0.05).

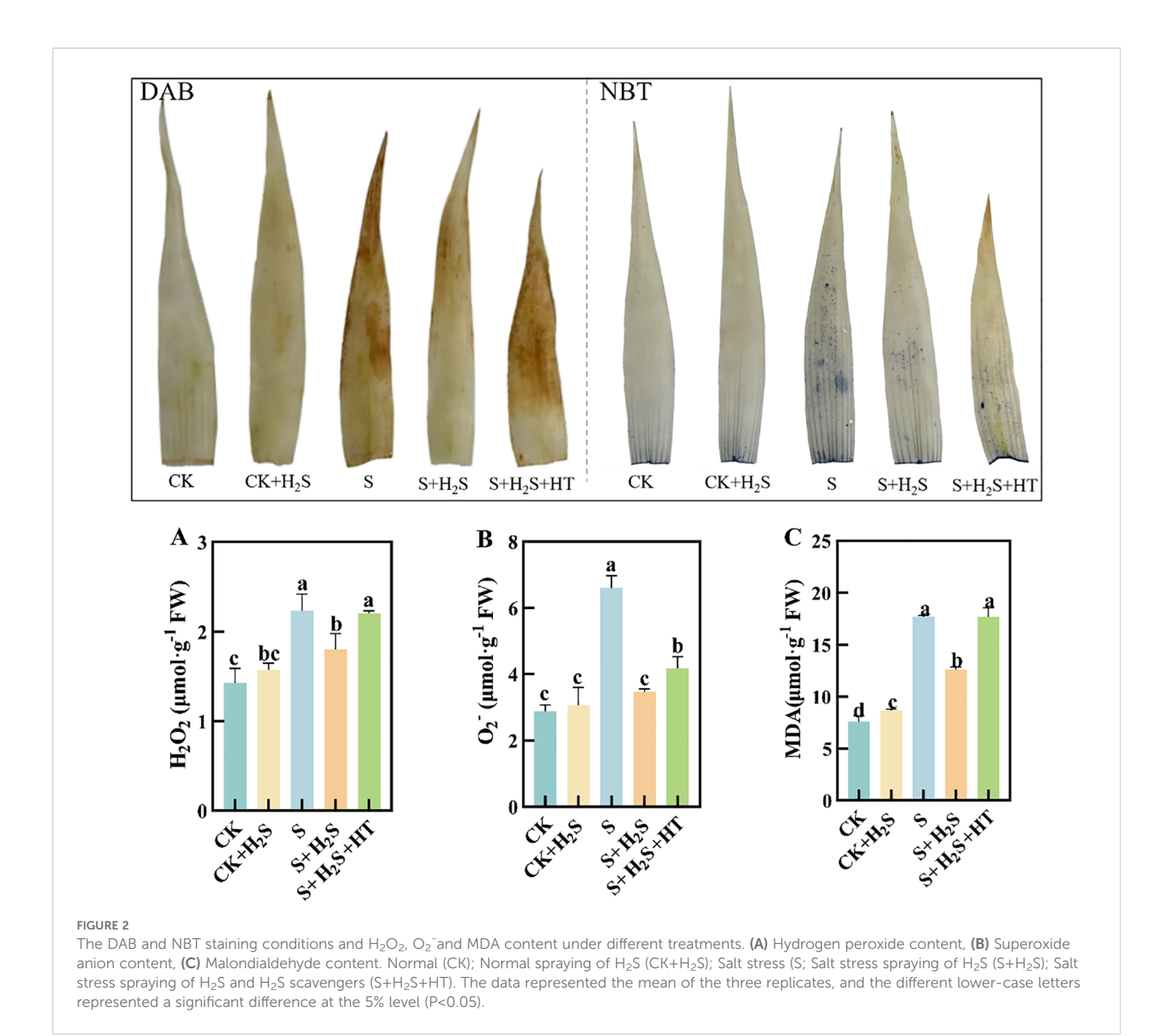
3.3 Effect of exogenous H₂S on the contents of AsA, DHA, GSH and GSSG in chloroplasts of sorghum seedlings

Salt stress significantly impaired the functioning of the AsA-GSH cycle within the chloroplasts of sorghum leaves at seedling stage. When compared to CK, the S treatment led to a significant reduction in the levels of AsA and GSH within the chloroplasts of sorghum seedling leaves, with decreases of 0.49% and 34.43% (P<0.05),

respectively (Figures 3A, B), while the contents of DHA and GSSG significantly decreased by 32.96% and 29.47%, respectively (Figures 3C, D). The S+H₂S treatment increased these contents by 5.72%, 23.77%, 17.22%, and 28.46%, respectively, compared to the S treatment. In contrast, the S+H₂S+HT treatment resulted in substantial declines in the levels of AsA, GSH, DHA, and GSSG by 18.47%, 26.15%, 11.36%, and 12.5%, respectively, when compared to the S+H₂S treatment.

3.4 Exogenous H₂S effectively increased APX, GR, DHAR and MDHAR activities in chloroplasts of sorghum seedlings

Salt stress notably suppressed the activity of enzymes involved in the AsA-GSH cycle (Figure 4). Compared to CK, the activities of APX, GR, DHAR, and MDHAR in the chloroplasts of sorghum seedling leaves under S treatment significantly decreased by 32.72%, 51.6%, 31.28%, and 30.65%, respectively. In contrast, the S+H₂S treatment resulted in substantial enhancements in the activities of APX, GR, DHAR, and MDHAR, with respective increases of 23.65%, 74.4%, 41.64%, and 31.88% compared to the S treatment. Furthermore, the S+H₂S+HT treatment significantly reduced the



activities of these enzymes by 26.19%, 66.59%, 50.51%, and 33.58%,

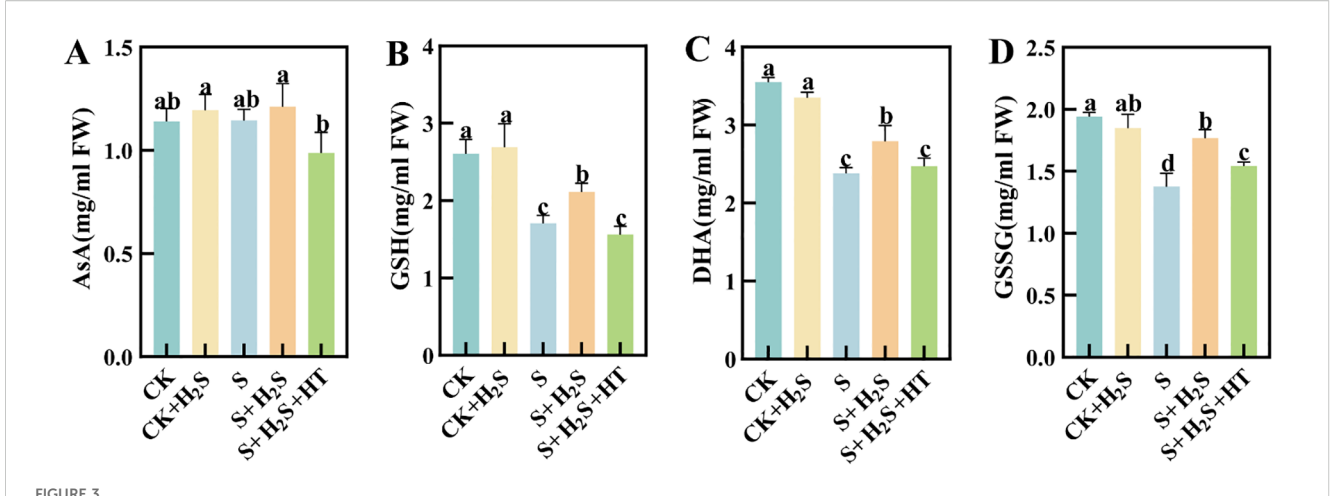
the foliar application of H₂S can alleviate the damage to the chloroplast respectively, when compared to the S+H₂S treatment. structure in sorghum seedling leaves caused by salt stress.

3.5 Effect of exogenous H₂S on chloroplast structure of sorghum seedlings

Transmission electron microscopy showed that chloroplasts in CKtreated seedling-age sorghum leaves were spindle-shaped, closely appressed against the cell walls, with intact double membrane structures and neatly stacked thylakoid grana that were clearly defined (Figure 5). In contrast, the chloroplasts under S treatment exhibited significant morphological alterations, with damaged chloroplast membranes and disorganized thylakoid grana, some of which were disintegrated and unclear. Compared to the S treatment, the S+H₂S treatment maintained the integrity of the double membrane structure, and the thylakoid grana were more orderly arranged. This suggested that

3.6 Effect of exogenous H₂S on chlorophyll synthesis precursor contents of sorghum seedlings

Salt stress led to elevated levels of ALA and PBG in sorghum seedling leaves (Figures 6A, B), while simultaneously reducing the contents of Protol IX, Mg-Protol IX, and Pchlide (Figures 6C-E). Compared to CK, the S treatment resulted in substantial increases in content of ALA and PBG by 76.06% and 29.96%, respectively. Conversely, the contents of Protol IX, Mg-Protol IX, and Pchlide significantly reduced by 29.3%, 32.39% and 23.78%, respectively. In comparison with the S treatment, the S+H₂S treatment significantly reduced the content of ALA and PBG in sorghum leaves at the seedling



Effects of H_2S spraying on chloroplast AsA, DHA, GSH, and GSSG contents of sorghum seedlings under salt stress **(A)** AsA content, **(B)** GSSG content, **(C)** DHA content, **(D)** GSSG content. Normal (CK): Normal spraying of H_2S (CK+ H_2S): Salt stress (S): Salt stress spraying of H_2S and H_2S scavengers (S+ H_2S +HT). The data represented the mean of the three replicates, and the different lower-case letters represented a significant difference at the 5% level (P<0.05).

stage by 26.61% and 22.53%, respectively, and increased the content of Protol IX, Mg-Protol IX, and Pchlide by 26.2%, 35.91%, and 21.3%, respectively. Furthermore, compared to the S+H₂S treatment, the S+H₂S+HT treatment increased the content of ALA and PBG by 30.35% and 10.33%, respectively, and significantly decreased the content of Protol IX (21.39%), Mg-Protol IX (34.89%), and Pchlide (24.51%).

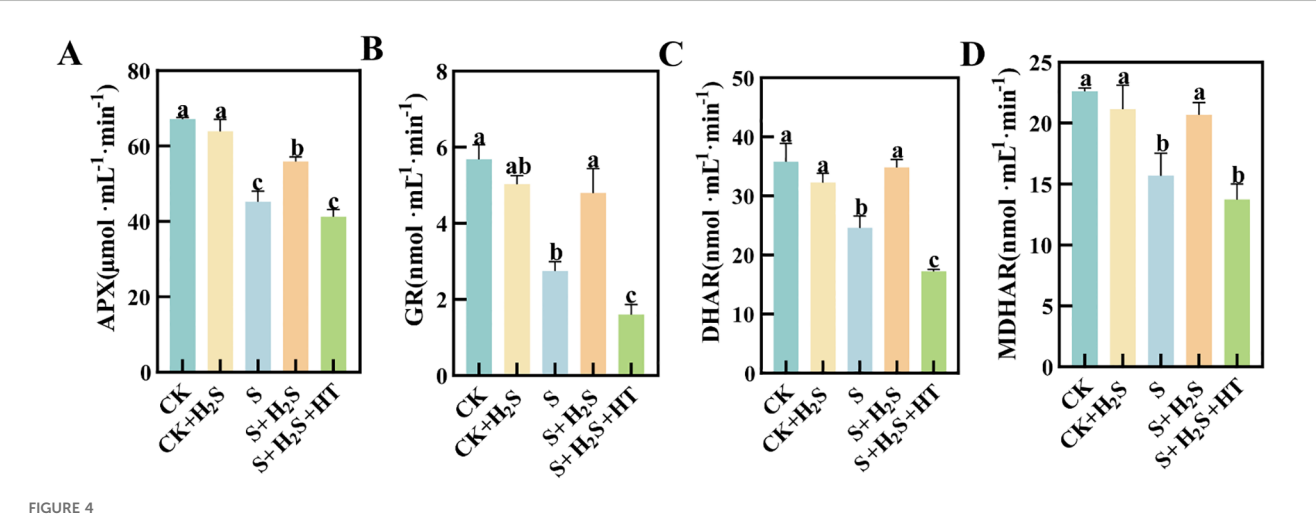
in the contents of Chla, Chlb, and Car by 46.56%, 30.64%, and 53.99%, respectively. In contrast, compared to the S treatment, the S+ H_2 S treatment resulted in notable increases in Chla (14.97%), Chlb (15.95%), and Car (34.21%). Furthermore, compared to the S+ H_2 S treatment, the S+ H_2 S+HT treatment caused a decrease in the contents of Chla (5.94%), Chlb (6.17%), and Car (10.19%).

3.7 Effect of exogenous H₂S on chloroplast Chla, Chlb and Car contents of sorghum seedlings

Under salt stress conditions, the concentrations of Chla, Chlb, and Car in the leaves of sorghum seedlings were substantially reduced (Figure 7). Compared to CK, S treatment led to substantial reductions

3.8 Effect of exogenous H₂S on chlorophyll fluorescence parameters of sorghum seedlings

The chlorophyll fluorescence parameters Fm and Fv/Fm in sorghum seedling leaves decreased, while F0 and NPQ increased when subjected to salt stress (Figure 8). Compared to CK, the Fm



Effects of H_2S spraying on chloroplast APX, GR, DHAR and MDHAR activities of sorghum seedlings under salt stress (A) APX activity, (B) GR activity, (C) MDHAR activity, (D) DHAR activity. Normal (CK): Normal spraying of H_2S (CK+ H_2S): Salt stress (S): Salt stress spraying of H_2S and H_2S according to the data represented the mean of the three replicates, and the different lower-case letters represented a significant difference at the 5% level (P<0.05).

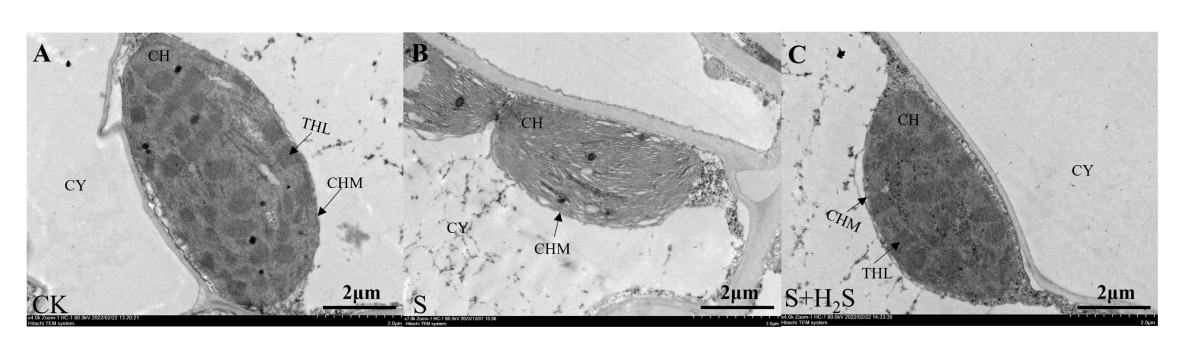


FIGURE 5 Effects of H_2S spraying on the ultrastructure of chloroplasts in sorghum seedlings under salt stress. (CY) cytoplasm, (CH) chloroplast, (CHM) chloroplast membrane, (THL) thylakoid lamella. (A-C) indicate normal (CK), Salt stress (S) and Effect of salt stress spray H_2S (S+ H_2S) on chloroplast ultrastructure (A-Dx7000 magnification, scale =2 μ m), respectively.

and Fv/Fm in the S treatment significantly decreased by 31.34% and 12.77%, respectively, while F0 and NPQ significantly increased by 20.01% and 76.66%, respectively. In comparison with the S treatment, the S+H₂S treatment reduced F0 and NPQ by 24.02% and 33.96%, respectively, and increased Fm and Fv/Fm by 22.47% and 9.1%, respectively. Furthermore, compared to the S+H₂S treatment, the S+H₂S+HT treatment led to a decrease in Fm and Fv/Fm by 20.44% and 7.95%, respectively, and an increase in F0 and NPQ by 34.15% and 4.71%, respectively.

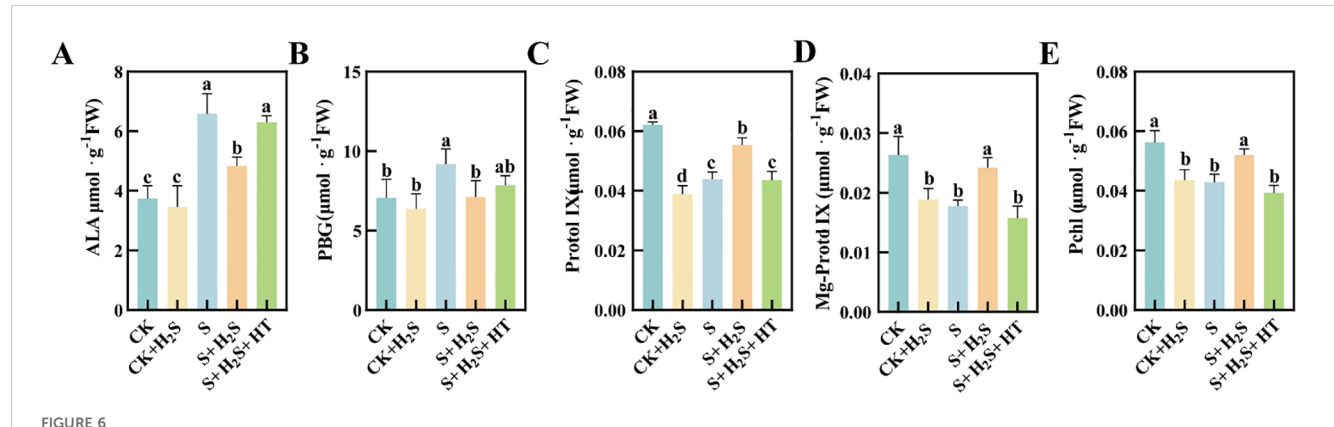
3.9 Effect of exogenous H₂S on gas exchange parameters of sorghum seedlings

Sorghum seedling leaves showed reduced Pn, Gs, and Tr (Figures 9A–C) under salt stress, while Ci increased (Figure 9D). S treatment compared to CK significantly reduced Pn, Gs and Tr in sorghum seedling leaves by 88.76%, 79.63%, and 85.23%, respectively, and Ci increased significantly by 49.72%. In contrast, the S+H₂S treatment significantly increased Pn, Gs and Tr by 351.02%, 144%, and 159.64%, separately, and significantly

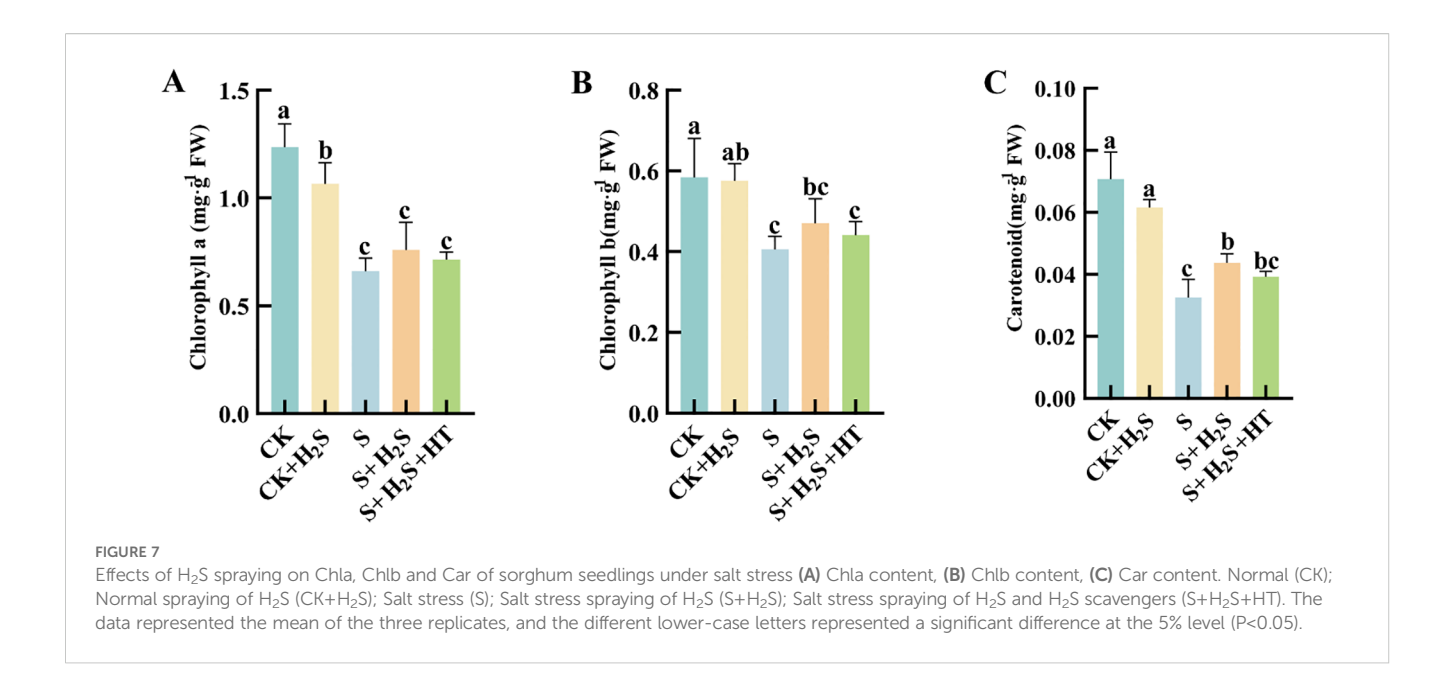
decreased Ci by 38.27% compared to the S treatment. Furthermore, compared to the S+H₂S treatment, the S+H₂S+HT treatment significantly reduced Pn, Gs and Tr by 90.49%, 81.78%, and 82.43%, respectively, and significantly increased Ci by 73.79%.

3.10 Impact of exogenous H₂S on OJIP curve and PQ pool in sorghum seedlings

Under salt stress, the shape of the OJIP curve of sorghum seedling leaves varied with the different treatments (Figure 10A). Compared to CK, the fluorescence signal intensity was significantly reduced in the S treatment. The S+H₂S treatment increased Compared with S treatment, the fluorescence signal intensity of sorghum leaves at seedling stage increased significantly. The fluorescence signal intensity of leaves treated with S+H₂S+HT showed no significant difference compared to the S treatment. However, the fluorescence signal intensity of leaves treated with S+H₂S was higher than that of the S+H₂S+HT treatment, particularly during the I-P phase, indicating a notable increase. Under salt stress, calculation of the MT and ST area ratio indicated a decrease in the PQ pool of sorghum seedling leaves (Figure 10B). Specifically, the size of the PQ pool was



Effects of H_2S spray on chlorophyll synthesis precursors of sorghum seedlings under salt stress (A) ALA, (B) PBG, (C) Protol IX, (D) Mg-Protol IX, (E) Pchl. Normal (CK): Normal spray H_2S (CK+ H_2S); Salt stress spray H_2S (S+ H_2S); Salt stress spray H_2S and H_2S scavenger (S+ H_2S +HT). The data represented the mean of the three replicates, and the different lower case letters represented a significant difference at the 5% level (P<0.05).

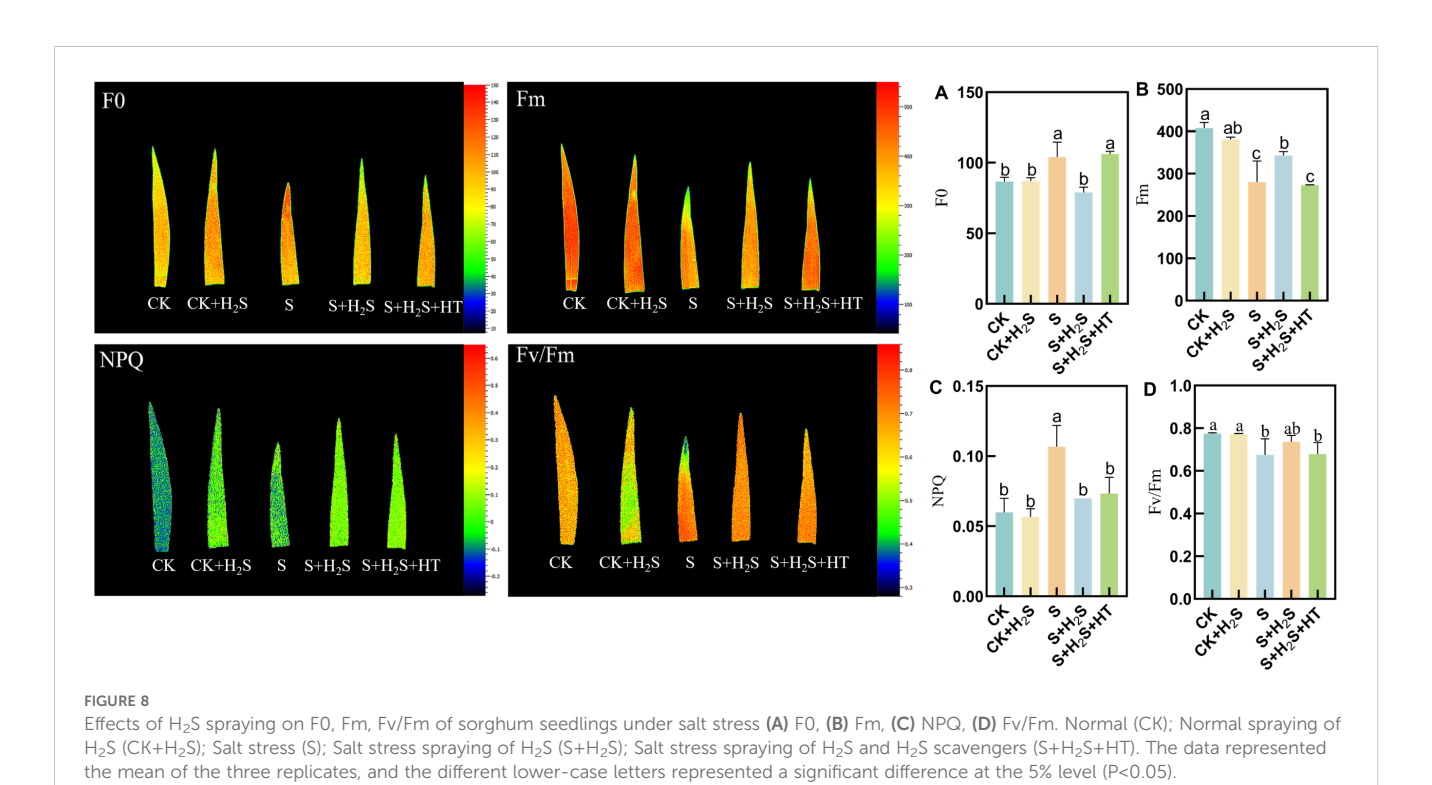


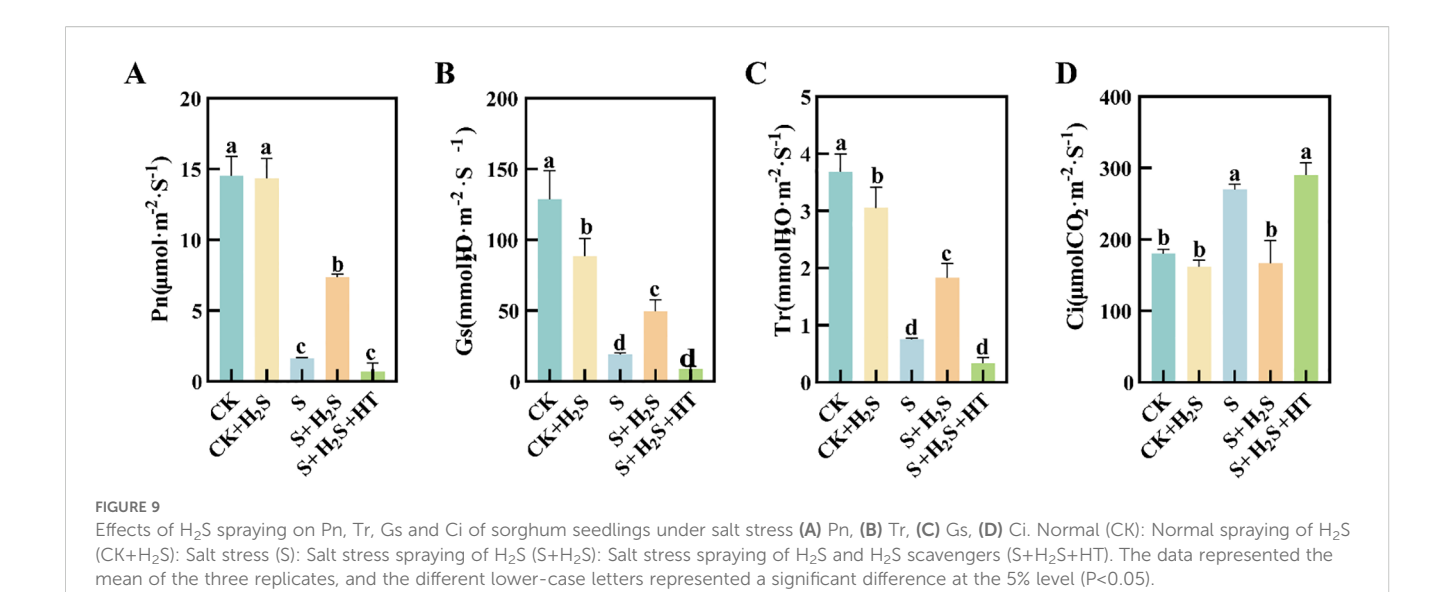
significantly diminished by 11.32% in the S treatment compared to the CK. Conversely, compared to the S treatment, the PQ pool size expanded by 3.01% in the S+H₂S treatment.

4 Discussion

Salt stress severely impeded the growth of sorghum seedlings, as manifested by the reduction in plant height, root length, and biomass accumulation compared with control plants. Such growth inhibition is a common outcome of osmotic and ionic stress, which limits cell expansion and nutrient acquisition. Similar inhibitory effects of salinity on plant growth have been widely reported (Van Zelm et al., 2020). However, exogenous H_2S application effectively alleviated these negative effects, highlighting its role as a growth-promoting factor under saline conditions. Conversely, the suppression of endogenous H_2S abolished these benefits, further confirming its protective role in sorghum growth under salt stress (Figure 1).

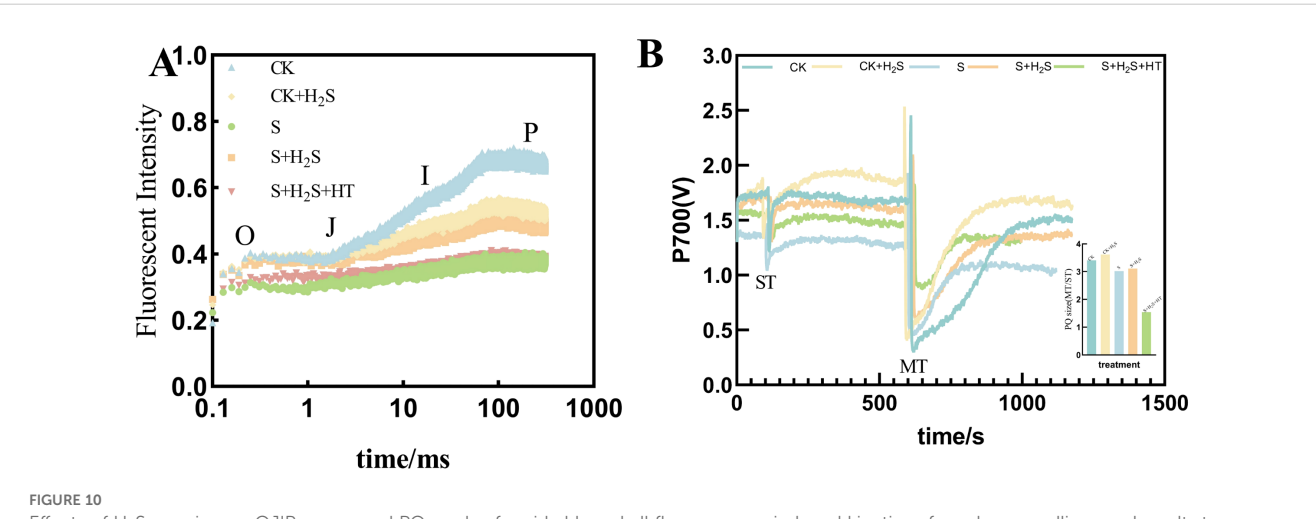
Photosynthesis is particularly vulnerable to salinity, and our findings demonstrate that salt stress led to a pronounced decline in



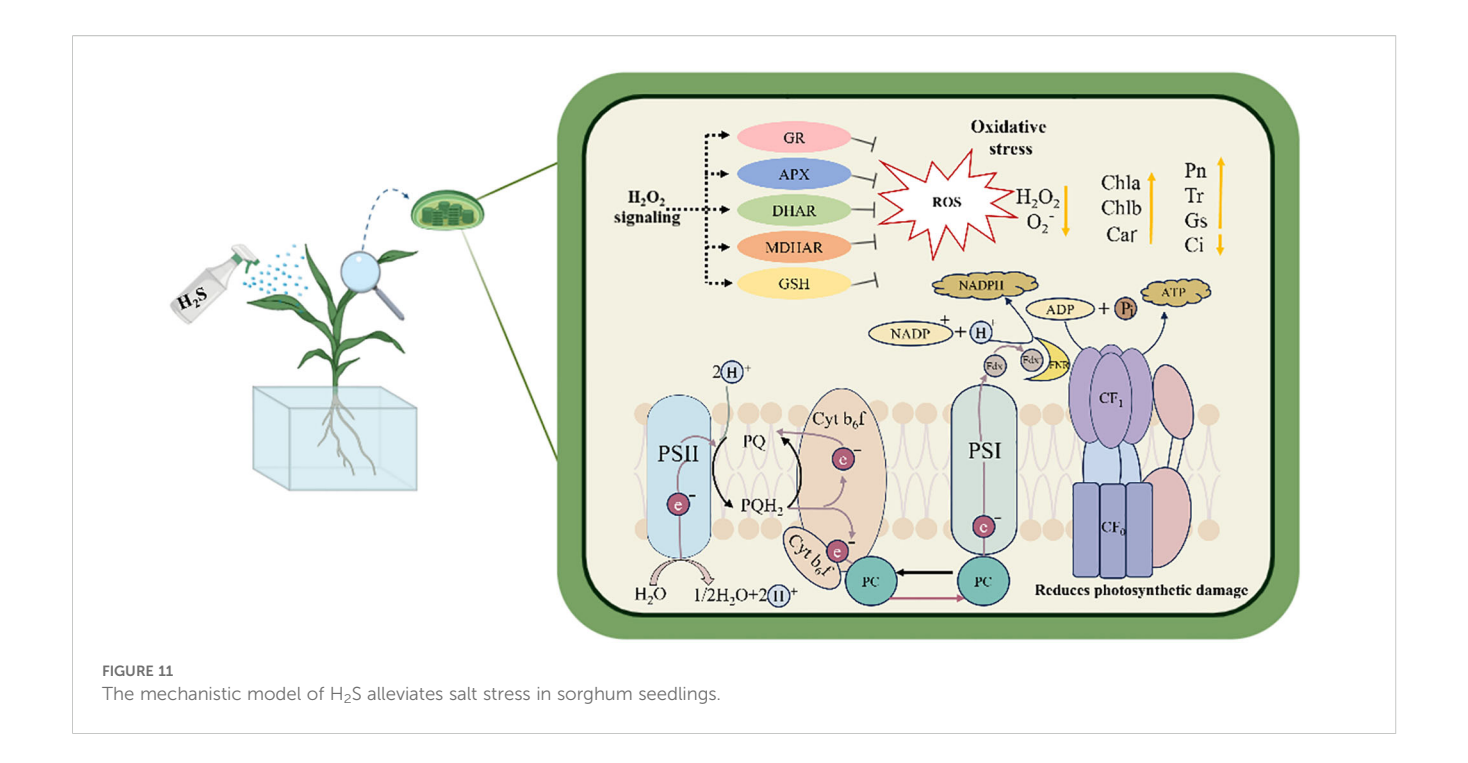


photosynthetic parameters, including net photosynthetic rate (Pn), stomatal conductance (Gs), and transpiration rate (Tr), along with an increase in intercellular CO₂ concentration (Ci). These changes indicate both stomatal and non-stomatal limitations to carbon assimilation, consistent with previous studies (Guo et al., 2018; Shen et al., 2024). Application of H₂S markedly restored these parameters, suggesting its role in enhancing photosynthetic efficiency under stress (Figure 9). This recovery may be attributed to the preservation of chlorophyll content and the stabilization of chloroplast ultrastructure. Salt stress is known to inhibit chlorophyll biosynthesis, leading to reduced Chla, Chlb, and Car contents (Kamran et al., 2020), whereas H₂S treatment prevented such declines, similar to earlier reports that H₂S protects chlorophyll from degradation under stress (Tang et al., 2020) (Figure 7). Furthermore, the increase in chlorophyll precursors such as Proto IX and Pchl after H₂S application aligns with evidence

that H₂S promotes chlorophyll synthesis (Wang et al., 2021). Importantly, chlorophyll fluorescence parameters, including Fm and Fv/Fm, which indicate PSII photochemical efficiency, were improved by H₂S (Figure 8). These results suggest that H₂S protects PSII from salt-induced damage, corroborated by the observed chloroplast ultrastructure integrity. Moreover, the reduction in signal fluorescence intensity under salt stress, implying impaired redox homeostasis and potential damage to the oxygen-evolving complex (Huang et al., 2019), was alleviated by H₂S, which facilitated electron transfer from PSII reaction centers to acceptors (QA, QB, PQ). A critical consequence of salt stress is the excessive accumulation of reactive oxygen species (ROS), including H₂O₂ and O₂-, which trigger oxidative damage as indicated by enhanced malondialdehyde (MDA) levels and positive DAB/NBT staining. This observation is consistent with earlier reports of ROS-induced cellular injury in plants under



Effects of H_2S spraying on OJIP curves and PQ pools of rapid chlorophyll fluorescence-induced kinetics of sorghum seedlings under salt stress (A) PQ library and (B) OJIP curves. Note: A single turnover saturation pulse analysis is performed to determine the P700 signal (ST), followed by a double turnover saturation pulse analysis (MT), the PQ library is oxidized, then the PQ size is MT area over ST area. Normal (CK); Normal spraying of H_2S (CK+ H_2S); Salt stress (S); Salt stress spraying of H_2S (S+ H_2S); Salt stress spraying of H_2S and H_2S scavengers (S+ H_2S +HT). The data represented the mean of the three replicates, and the different lower-case letters represented a significant difference at the 5% level (P<0.05).



salinity (Ozfidan-Konakci et al., 2020; Meng et al., 2024). In our study, H_2S significantly reduced ROS and lipid peroxidation markers, thereby mitigating oxidative stress in sorghum seedlings (Figure 2). This reduction suggests that H_2S not only restricts ROS overproduction but also enhances the detoxification mechanisms required to maintain cellular redox balance.

The observed alleviation of oxidative stress by H₂S is closely linked to its regulatory effect on antioxidant metabolism. Under salt stress, the contents of ascorbate (AsA) and glutathione (GSH), as well as their oxidized counterparts (DHA and GSSG), declined, indicating disruption of the ascorbate-glutathione (AsA-GSH) cycle (Chauhan et al., 2021; Bashir et al., 2022; Tan et al., 2022) (Figure 3). Additionally, the activities of key enzymes, including APX, GR, DHAR, and MDHAR, were suppressed, further weakening the redox buffering capacity (Figure 4). Previous studies have shown that these enzymes are regulated by stress signals and are essential for detoxifying ROS (Pallavi et al., 2012; Jahan et al., 2019), while overexpression of APX in transgenic plants enhances oxidative stress tolerance (Gill and Tuteja, 2010). In our study, exogenous H₂S restored both the metabolite pools and enzymatic activities, thereby reactivating the AsA-GSH cycle. Furthermore, the cross-talk between the AsA-GSH cycle and other antioxidant systems such as thioredoxin and glutaredoxin may contribute to the overall redox homeostasis (Wu et al., 2019; Luo et al., 2023). Collectively, these findings demonstrate that H2S enhances sorghum tolerance to salinity by integrating growth regulation, photosynthetic protection, ROS scavenging, and antioxidant metabolism.

5 Conclusion

This study demonstrated that under salt stress, exogenous application of H₂S effectively alleviated oxidative stress in sorghum

seedlings by activating the AsA-GSH cycle within chloroplasts, thereby maintaining cellular redox homeostasis. Meanwhile, H₂S preserved chlorophyll content and chloroplast ultrastructure, improved chlorophyll fluorescence parameters, protected photosystem II (PSII) from damage, and facilitated electron transfer from the PSII reaction center to plastoquinone. Collectively, these effects enhanced photosynthetic performance, ultimately mitigating the adverse impacts of salt stress on sorghum seedlings (Figure 11).

Data availability statement

The original contributions presented in the study are included in the article/supplementary material. Further inquiries can be directed to the corresponding author.

Author contributions

CL: Project administration, Writing – original draft. SL: Data curation, Investigation, Writing – review & editing. XH: Data curation, Investigation, Writing – review & editing. XS: Writing – review & editing. CJL: Writing – review & editing. LS: Writing – review & editing. YZ: Project administration, Supervision, Writing – review & editing.

Funding

The author(s) declare financial support was received for the research and/or publication of this article. This work was financially supported by the China Agriculture Research System of MOF and MARA (CARS-06-14.5-A17) and the Major Project of Food Crop

Production Based on Technological Application of Liaoning Province (2023JH1/10200001-03-01).

Conflict of interest

The authors declare that the research was conducted in the absence of any commercial or financial relationships that could be construed as a potential conflict of interest.

Generative AI statement

The author(s) declare that no Generative AI was used in the creation of this manuscript.

Any alternative text (alt text) provided alongside figures in this article has been generated by Frontiers with the support of artificial intelligence and reasonable efforts have been made to ensure accuracy, including review by the authors wherever possible. If you identify any issues, please contact us.

Publisher's note

All claims expressed in this article are solely those of the authors and do not necessarily represent those of their affiliated organizations, or those of the publisher, the editors and the reviewers. Any product that may be evaluated in this article, or claim that may be made by its manufacturer, is not guaranteed or endorsed by the publisher.

References

Alvi, A. F., Iqbal, N., Albaqami, M., and Khan, N. A. (2023). The emerging key role of reactive sulfur species in abiotic stress tolerance in plants. *Physiol. Plant* 175, e13945. doi: 10.1111/ppl.13945

Bashir, S., Jan, N., Wani, U. M., Raja, N., and John, R. (2022). Co-over expression of Ascorbate Glutathione pathway enzymes improve mercury tolerance in tomato. *Plant Physiol. Biochem.* 186, 170–181. doi: 10.1016/j.plaphy.2022.07.015

Bhattacharya, O., Ortiz, I., and Walling, L. L. (2020). Methodology: an optimized, high-yield tomato leaf chloroplast isolation and stroma extraction protocol for proteomics analyses and identification of chloroplast co-localizing proteins. *Plant Methods* 16, 131. doi: 10.1186/s13007-020-00667-5

Bogorad, L. (1962). Porphyrin synthesis. In *Methods in Enzymology*, Vol. 5, 885–895. Academic Press.

Chauhan, D. K., Yadav, V., Vaculik, M., Gassmann, W., Pike, S., Arif, N., et al. (2021). Aluminum toxicity and aluminum stress-induced physiological tolerance responses in higher plants. *Crit. Rev. Biotechnol.* 41, 715–730. doi: 10.1080/07388551.2021.1874282

Chen, X., Zhang, R., Li, B., Li, B., Cui, T., Liu, C., et al. (2022). Alleviation of oxidative damage induced by caCl₂ priming is related to osmotic and ion stress reduction rather than enhanced antioxidant capacity during germination under salt stress in sorghum. *Front. Plant Sci.* 13, 881039. doi: 10.3389/fpls.2022.881039

Cui, J., Li, C., Qi, J., Yu, W., and Li, C. (2025). Hydrogen sulfide in plant cold stress: functions, mechanisms, and challenge. *Plant Mol. Biol.* 115, 12. doi: 10.1007/s11103-024-01535-9

Gill, S. S., and Tuteja, N. (2010). Reactive oxygen species and antioxidant machinery in abiotic stress tolerance in crop plants. *Plant Physiol. Biochem.* 48, 909–930. doi: 10.1016/j.plaphy.2010.08.016

Guo, L. L., Hao, L. H., Jia, H. H., Li, F., Zhang, X.X., Cao, X., et al. (2018). Effects of NaCl stress on stomatal traits, leaf gas exchange parameters, and biomass of two tomato cultivars. *Ying. Yong. Sheng. Tai. Xue. Bao.* 29, 3949–3958. doi: 10.13287/j.1001-9332.201812.022

Guo, X., Zhi, W., Feng, Y., Zhou, G., and Zhu, G. (2022). Seed priming improved salt-stressed sorghum growth by enhancing antioxidative defense. *PloS One* 17, e0263036. doi: 10.1371/journal.pone.0263036

Huang, L.-Y., Li, Z.-Z., Duan, T.-Y., Wang, L., Zhang, Y.Q., and Li, J. (2019). Regulation of exogenous calcium on photosynthetic system of honeysuckle under salt stress. *Zhongguo Zhong Yao Za Zhi* 44, 1531–1536. doi: 10.19540/j.cnki.cjcmm.20190322.101

Jahan, M. S., Shu, S., Wang, Y., Chen, Z., He, M., Tao, M., et al. (2019). Melatonin alleviates heat-induced damage of tomato seedlings by balancing redox homeostasis and modulating polyamine and nitric oxide biosynthesis. *BMC Plant Biol.* 19, 414. doi: 10.1186/s12870-019-1992-7

Jin, M., Wang, H., Liu, H., Xia, Y., Ruan, S., Huang, Y., et al. (2020). Oxidative stress response and proteomic analysis reveal the mechanisms of toxicity of imidazolium-based ionic liquids against *Arabidopsis thaliana*. *Environ. Pollut.* 260, 114033. doi: 10.1016/j.envpol.2020.114033

Kamran, M., Xie, K., Sun, J., Wang, D., Shi, C., Lu, Y., et al. (2020). Modulation of growth performance and coordinated induction of ascorbate-glutathione and methylglyoxal detoxification systems by salicylic acid mitigates salt toxicity in choysum (*Brassica parachinensis* L.). *Ecotoxicol. Environ. Saf.* 188, 109877. doi: 10.1016/j.ecoenv.2019.109877

Kaya, C. (2021). Salicylic acid-induced hydrogen sulphide improves lead stress tolerance in pepper plants by upraising the ascorbate-glutathione cycle. *Physiol. Plant.* 173 (1), 8–19. doi: 10.1111/ppl.13434

Khan, M. N., Mukherjee, S., Al-Huqail, A. A., Basahi, R. A., Ali, H. M., Al-Munqedhi, B. M. A., et al. (2021). Exogenous potassium (K $^+$) positively regulates Na $^+$ /H $^+$ antiport system, carbohydrate metabolism, and ascorbate-glutathione cycle in H₂₊S-dependent manner in NaCl-stressed tomato seedling roots. *Plants* 10(5), 948. doi: 10.3390/plants10050948

Liang, Z., Shi, S., Xue, B., Li, D., Liu, Y., and Liu, C. (2025). Comparative analysis of TALE gene family in gramineae. Agronomy 15, 1460. doi: 10.3390/agronomy15061460

Liu, C., Tian, L., Yu, W., Wang, Y., Yao, Z., Liu, Y., et al. (2024). Natural variation in *SbTEF1* contributes to salt tolerance in sorghum seedlings. *J. Integr. Agric.* doi: 10.1016/j.jia.2024.03.030

Liu, J., Wu, Y., Dong, G., Zhu, G., and Zhou, G. (2023). Progress of research on the physiology and molecular regulation of sorghum growth under salt stress by gibberellin. *Int. J. Mol. Sci.* 24 (7), 6777. doi: 10.3390/ijms24076777

Luo, S., Liu, Z., Wan, Z., He, X., Lv, J., Yu, J., et al. (2023). Foliar spraying of NaHS alleviates cucumber salt stress by maintaining $\rm Na^+/K^+$ balance and activating salt tolerance signaling pathways. *Plants* 12 (13), 2718. doi: 10.3390/plants12132718

Meng, F., Feng, N., Zheng, D., Liu, M., Zhou, H., Zhang, R., et al. (2024). Exogenous Hemin enhances the antioxidant defense system of rice by regulating the AsA-GSH cycle under NaCl stress. *Peerj* 12, e17219. doi: 10.7717/peerj.17219

Mishra, A. K., Das, R., George Kerry, R., Biswal, B., Sinha, T., Sharma, S., et al. (2023). Promising management strategies to improve crop sustainability and to amend soil salinity. *Front. Environ. Sci.* 10. doi: 10.3389/fenvs.2022.962581

Moloi, M. J., and van der Westhuizen, A. J. (2006). The reactive oxygen species are involved in resistance responses of wheat to the Russian wheat aphid. *J. Plant Physiol.* 163 (11), 1118–1125. doi: 10.1016/j.jplph.2005.11.003

Ozfidan-Konakci, C., Yildiztugay, E., Alp, F. N., Kucukoduk, M., and Turkan, I. (2020). Naringenin induces tolerance to salt/osmotic stress through the regulation of nitrogen metabolism, cellular redox and ROS scavenging capacity in bean plants. *Plant Physiol. Biochem.* 157, 264–275. doi: 10.1016/j.plaphy.2020.10.032

Pallavi, S., Bhushan, J. A., Shanker, D. R., and Mohammad, P. (2012). Reactive oxygen species, oxidative damage, and antioxidative defense mechanism in plants under stressful conditions. *J. Bot.* 2012, 1–26. doi: 10.1155/2012/217037

Parihar, P., Singh, S., Singh, R., Singh, V. P., and Prasad, S. M. (2015). Effect of salinity stress on plants and its tolerance strategies: a review. *Environ. Sci. pollut. Res.* 22, 4056–4075. doi: 10.1007/s11356-014-3739-1

Prajapati, P., Gupta, P., Kharwar, R. N., and Seth, C. S.. (2023). Nitric oxide mediated regulation of ascorbate-glutathione pathway alleviates mitotic aberrations and DNA damage in Allium cepa L. under salinity stress. *Int. J. Phytoremediation* 25(4), 403–414. doi: 10.1080/15226514.2022.2086215

Rajabi Dehnavi, A., Zahedi, M., Ludwiczak, A., and Piernik, A. (2022). Foliar application of salicylic acid improves salt tolerance of sorghum (*Sorghum bicolor L.*) moench). *Plants-Basel* 11, 368. doi: 10.3390/plants11030368

Shen, X., Sun, M., Nie, B., and Li, X. (2024). Physiological adaptation of Cyperus esculentus L. seedlings to varying concentrations of saline-alkaline stress: Insights from photosynthetic performance. *Plant Physiol. Biochem.* 214, 108911. doi: 10.1016/j.plaphy.2024.108911

Subba, R., Dey, S., Mukherjee, S., Roy, S., and Mathur, P. (2023). Elucidating the role of exogenous iron (Fe) in regulation of hydrogen sulphide (H_2S) biosynthesis and its concomitant effect on seedling growth, pigment composition and antioxidative defense in NaCl-stressed tomato seedlings. *Acta Physiol. Plant.* 45 (12), 135. doi: 10.1007/s11738-023-03561-7

Tan, Z., Xuan, Z., Wu, C., Cheng, Y., Xu, C., Ma, X., et al. (2022). Effects of selenium on the as A-GSH system and photosynthesis of pakchoi (*Brassica chinensis* L.) under lead stress. *J. Soil Sci. Plant Nutr.* 22, 5111–5122. doi: 10.1007/s42729-022-00987-6

Tang, X., An, B., Cao, D., Xu, R.Wang S., Zhang, Z., et al. (2020). Improving photosynthetic capacity, alleviating photosynthetic inhibition and oxidative stress under low temperature stress with exogenous hydrogen sulfide in blueberry seedlings. *Front. Plant Sci.* 11, 108. doi: 10.3389/fpls.2020.00108

Tao, Y., Trusov, Y., Zhao, X., Wang, X., Cruickshank, A.W., Hunt, C., et al. (2021). Manipulating assimilate availability provides insight into the genes controlling grain size in sorghum. *Plant J.* 108, 231–243. doi: 10.1111/tpj.15437

Thakur, M., Anand, A., and Hydrogen sulfide: 2021 (2021). An emerging signaling molecule regulating drought stress response in plants. *Physiol. Plantarum* 172, 1227–1243. doi: 10.1111/ppl.13432

Van Zelm, E., Zhang, Y., and Testerink, C. (2020). Salt tolerance mechanisms of plants. In S. S. Merchant (Ed.), *Annu. Rev. Plant Biol.* 71, 403–433. doi: 10.1146/annurey-arplant-050718-100005

Wang, P., Yin, L., Liang, D., Li, C., Ma, F., and Yue, Z. (2012). Delayed senescence of apple leaves by exogenous melatonin treatment: toward regulating the ascorbate-glutathione cycle. *J. Pineal Res.* 53 (1), 11–20. doi: 10.1111/j.1600-079X.2011.00966.x

Wang, H., Liu, Z., Luo, S., Li, J., Zhang, J., Li, L., et al. (2021). 5-Aminolevulinic acid and hydrogen sulphide alleviate chilling stress in pepper (*Capsicum annuum* L.) seedlings by enhancing chlorophyll synthesis pathway. *Plant Physiol. Biochem.* 167, 567–576. doi: 10.1016/j.plaphy.2021.08.031

Wang, J., Dou, J., Yue, Z., Wang, J., Chen, T., Li, J., et al. (2024). Effect of hydrogen sulfide on cabbage photosynthesis under black rot stress. *Plant Physiol. Biochem.* 208, 108453. doi: 10.1016/j.plaphy.2021.108453

Wei, C., Gao, L., Xiao, R., Wang, Y., Chen, B., Zou, W., et al. (2024). Complete telomere-to-telomere assemblies of two sorghum genomes to guide biological discovery. *Imeta* 3, e193. doi: 10.1002/imt2.193

Wu, Y., Jin, X., Liao, W., Hu, L., Dawuda, M. M., Zhao, X., et al. (2018). 5-Aminolevulinic acid (ALA) alleviated salinity stress in cucumber seedlings by enhancing chlorophyll synthesis pathway. *Front. Plant Sci.* 9, 635. doi: 10.3389/fpls.2018.00635

Wu, Y., Hu, L., Liao, W., Dawuda, M.M., Lyu, J., Xie, J., et al. (2019). Foliar application of 5-aminolevulinic acid (ALA) alleviates NaCl stress in cucumber (*Cucumis sativus* L.) seedlings through the enhancement of ascorbate-glutathione cycle. *Sci. Hortic.* 257, 108761. doi: 10.1016/j.scienta.2019.108761

Xuan, L., Li, J., Wang, X., and Wang, C. (2020). Crosstalk between hydrogen sulfide and other signal molecules regulates plant growth and development. *Int. J. Mol. Sci.* 21, 4593. doi: 10.3390/ijms21134593

Xue, B., Liang, Z., Li, D., Liu, Y., and Liu, C. (2024a). Genome-wide identification and expression analysis of *CASPL* gene family in *Zea mays* (L.). *Front. Plant Sci.* 15, 1477383. doi: 10.3389/fpls.2024.1477383

Xue, B., Liang, Z., Liu, Y., Li, D., Cao, P., and Liu, C. (2024b). Comparative Analysis of Casparian Strip Membrane Domain Protein Family in *Oryza sativa* (L.) and *Arabidopsis thaliana* (L.). *Int. J. Mol. Sci.* 25, 9858. doi: 10.3390/ijms25189858

Xue, B., Liang, Z., Liu, Y., Li, D., and Liu, C. (2024c). Genome-Wide Identification of the *RALF* Gene Family and Expression Pattern Analysis in *Zea mays* (L.) under Abiotic Stresses. *Plants* 13, 2883. doi: 10.3390/plants13202883

Yang, Z., Li, J. L., Liu, L. N., Xie, Q., and Sui, N. (2020). Photosynthetic regulation under salt stress and salt-tolerance mechanism of sweet sorghum. *Front. Plant Sci.* 10, 1722. doi: 10.3389/fpls.2019.01722

Yu, W., Li, D., Liu, C., Xu, J., Yan, J., Cao, P., et al. (2025). Screening and Identification of Grain Sorghum Germplasm for salt tolerance at Seedling Stage. *Front. Plant Sci.* 16, 1610685. doi: 10.3389/fpls.2025.1610685

Yu, W., Wang, Y., Hu, L., Shi, X., Huang, Y., Liu, C., et al. (2024). The identification of *kabatiella zeae* as a causal agent of northern anthracnose of sorghum in China and estimation of host resistance. *Plants* 13, 1857. doi: 10.3390/plants13131857

Zhang, T., Gong, H., Wen, X., and Lu, C. (2010). Salt stress induces a decrease in excitation energy transfer from phycobilisomes to photosystem I but an increase to photosystem I in the cyanobacterium Spirulina platensis. *J. Plant Physiol.* 167, 951–958. doi: 10.1016/j.jplph.2009.12.020

Zhu, L., Yu, H., Dai, X., Yu, M., and Yu, Z. (2022). Effect of methyl jasmonate on the quality and antioxidant capacity by modulating ascorbate-glutathione cycle in peach fruit. *Sci. Hortic.* 303, 111216. doi: 10.1016/j.scienta.2022.111216